The morphology of polyethylenes produced by alumina-supported zirconium tetrabenzyl

A. Akar*, N. C. Billingham and P. D. Calvert
School of Chemistry and Molecular Sciences, University of Sussex, Falmer, Brighton BN1 9QJ, UK
(*Received* 12 *February* 1982; *revised* 7 *February* 1983)

The morphology of the beads of polymer produced by polymerization of ethylene with an alumina-supported zirconium tetrabenzyl catalyst has been studied as a function of conversion. Before polymerization starts the alumina is in the form of spherical particles of diameter 20–70 μm made up of porous aggregates of subparticles of diameter 0.1–0.6 μm. Polymerization causes these particles to expand to form hollow, spherical beads of polymer whose inner walls contain clusters of alumina subparticles whose occurrence decreases with conversion. As the conversion increases there is considerable fissuring of the beads and at high conversions the walls are made up of 'worms' of polymer connecting clusters of catalyst subparticles; these worms have diameters of around 0.6 μm and are very similar to those observed from a wide variety of related catalyst systems. Differential scanning calorimetry analysis and optical microscopy of the polymer beads show a high melting temperature, a rapid increase in melting temperature with heating rate, delayed loss of birefringence in the melt and a rapid reversion to normal behaviour on nitric acid treatment, suggesting that the polymer is formed in a highly drawn state. It is proposed that the observed morphology arises from the interaction of monomer diffusion rate and polymerization rate. Using estimates for the diffusion rate of ethylene under various conditions it is shown that the observed morphology is consistent with a process which becomes diffusion controlled quite early in the reaction so that hollow beads are formed. With increasing conversion, expansion of the outer layers of the bead causes drawing and the production of worms. At the same time fissuring of the surface allows the ingress of monomer into the interior of the beads whose walls grow relatively uniformly at higher conversions.

Keywords Morphology; polyolefins; supported catalysts; metal alkyls; diffusion control; zirconium tetrabenzyl; alumina

INTRODUCTION

High-density polyethylene and polypropylene are both produced commercially using transition-metal catalysts that are heterogeneous. At the same time, the polymers produced are insoluble in the reaction medium, so that the reactions are heterogeneous with respect both to catalyst and to polymer. Since both polymers are semi-crystalline, they form with definite morphologies and the so-called 'nascent' morphology has been much studied, since it is usually accepted to represent a unique state in which the polymer chain is formed concurrently with its crystallization. In recent years the trend in plastics technology has been to use the as-polymerized powder for direct blending with pigments and additives so that the ability to understand and to control the size, shape and morphology of nascent polymer particles is industrially important.

Boor[1] has extensively reviewed nascent morphologies produced by Ziegler–Natta catalysts and there is an earlier review by Chanzy *et al.*[2] Experiments made at very low conversions suggest that the first recognizable structures which form on the catalyst surface in the early stages of polymerization are polymer globules formed mainly on edges, cracks and voids in the catalyst surface and sometimes developing quite rapidly into fibrils of about 20–100 nm diameter and indeterminate length. The structure of these fibrils is still not certain although it appears that they contain crystals with a range of melting behaviour, often identified as both folded-chain and extended-chain crystals. Most observations in the early stages of polymerization have been made by electron microscopy of polymers formed from the gas phase, including some experiments in which polymerization proceeds directly in the electron microscope[3,4] and their extrapolation to liquid-phase reactions must be viewed with caution. At higher conversions, in liquid-phase experiments, a common feature of many polyolefins produced by Ziegler–Natta catalysts is the formation of fibres having a diameter of ~0.5–1.0 μm and formed both irregularly twisted and helically coiled. Wristers[5] has reported extensive studies of these worm-like structures and suggests that they are the basic morphological unit of polymer particles at high conversion and that their formation is determined by the primary catalyst particles.

Fibrous morphologies are extremely common in Ziegler–Natta polymerizations and are often observed in the form of 'cobweb' structures in which the fibres form a three-dimensional interconnecting network with globules of polymer at the intersection. Graf *et al.*[6] suggested that these fibres are formed by the deformation associated with the increasing volume of the aggregate of catalyst particles during polymerization. Similar structures have been observed by Chanzy *et al.*[7] during polymerization of ethylene on a Ziegler–Natta catalyst system supported on the surface of starch granules.

* Present address: ITU Kimya Fakultesi, Agazaga Kampusu, Emirgan, Istanbul, Turkey

0032-3861/83/070889-09$03.00

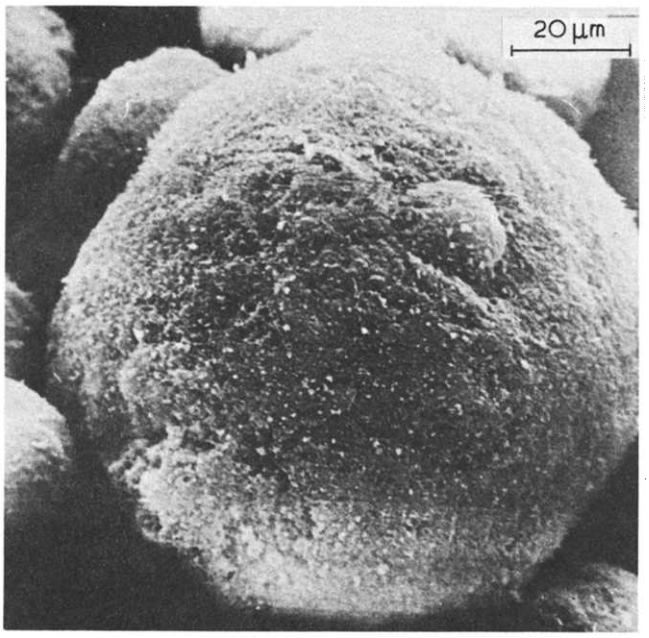

Figure 1 SEM photograph of alumina before polymerization

Although Ziegler–Natta catalysts have been most widely studied, ethylene is frequently polymerized by other catalyst systems, notably those consisting of transition-metal complexes supported on the surface of silica or alumina. Davidson[8] studied ethylene polymerization initiated by a silica-supported chromium catalyst and observed that fractured polymer granules consist of worms of polymer with a diameter of 0.5–0.9 μm which are coiled into helices; in scanning electron micrographs these coiled worms are almost identical to the structures observed by Wristers for propylene polymerization. More recently, Ballard[9] has reviewed the highly efficient catalysts for ethylene polymerization invented by his group[10] and produced by the reaction of stable transition-metal alkyl and allyl complexes with the hydroxyl groups on alumina or silica surfaces. These catalysts, especially those formed from reaction of zirconium tetrabenzyl with alumina, are commercially interesting because of their activity. At the same time their relatively well characterized structures and the availability of the unsupported materials as pure compounds, stable in inert atmospheres at room temperature, makes them attractive for scientific study. Ballard[11,12] and Murray[13,14] have described the morphology of polyethylenes produced by zirconium tetrabenzyl on alumina. They find that the polymer is produced in helical worms apparently identical to those produced by Ziegler–Natta and by supported chromium catalysts. Based on electron diffraction measurements[14] it is suggested[12] that the worms consist of stacks of chain-folded lamellar single crystals stacked with their long axes parallel to the axis of the worm.

Murray[14] has also reported that cobweb-like morphologies similar to those observed by others[6,7] can be formed on these catalysts at low conversions.

Although the initial morphologies of nascent polymers are variable and complex, the formation of worm-like entities of 0.5–1 μm diameter in polymerizations at moderate to high conversion seems to be a common feature of many different heterogeneous catalysts for olefin polymerization. Broadly speaking, three different mechanisms have been proposed to account for worm-like morphologies. Those authors who observe worms as parts of cobweb morphologies have usually ascribed their formation to mechanical deformation of the polymer during its formation. In contrast, Wristers[5] and others have proposed a root-growth mechanism in which the worms are envisaged as propagating from the surface of the catalyst particle, whilst Ballard[10] proposes a tip-growth mechanism in which growth occurs from a small particle of catalyst located in the tip of the worm. These latter two mechanisms become indistinguishable if the catalyst particle becomes small enough (less than the diameter of the worm), although no author seems to have any very convincing explanation of how polymerization at a small particle can lead to a worm-like structure rather than isotropic spherical growth.

Whatever the observed morphology, the close similarity between polymers formed from ethylene, propylene and higher olefins on a very wide range of polymerization catalysts suggest a common mechanism for morphological control and it seems most probable that this is a transport mechanism rather than a chemical mechanism. In this paper we report some studies of the polymerization of ethylene on alumina-supported zirconium catalysts in which we have examined the polymer morphology and attempted to elucidate the factors which determine it.

EXPERIMENTAL

Preparation and characterization of catalysts

Zirconium tetrabenzyl ($ZrBz_4$) was prepared by the reaction of benzyl magnesium chloride with zirconium tetrachloride, as described by Giannini and Zucchini[15]. The product was isolated by evaporation of the ether solvent and extraction of the dark precipitate with hexane/toluene mixtures. The extract was freed of magnesium by filtration through activated alumina, concentrated by evaporation, then the pure product crystallized at low temperature (−20°C) and twice recrystallized from toluene. All manipulations were performed in vacuum or in nitrogen-filled apparatus. Polymerization solvents (usually toluene) were distilled from calcium hydride or from zirconium tetrabenzyl before use. Ethylene monomer (polymerization grade) was donated by ICI Plastics Division and was used as supplied.

The alumina used for supporting the catalysts was Ketjen grade B, dried at 500°C before use. *Figure 1* shows a scanning electron micrograph of a typical alumina particle. The particles are spherical and about 90% have diameters in the range 20–70 μm. They consist of a porous aggregate of subparticles of about 0.1–0.6 μm diameter. Transmission electron microscopy of the sub-particles after ultrasonic disruption of the alumina showed that the subparticles are, in themselves, aggregates of primary particles with dimensions around 10 nm. X-ray diffraction measurements showed that the alumina produced by dehydration at 500°C for 10 h has the expected cubic, γ-alumina structure[16].

As a check on the uniform reactivity of the alumina particles some of the alumina was suspended in toluene and titrated with methyl red until the toluene remained slightly coloured. The alumina was recovered and dried and the particles broken open under an optical microscope. It was found that the alumina was uniformly stained

Table 1 Polymerization conditions and polymer properties

[Alumina] (g l^{-1})	PC_2H_4 (kg cm^{-2})	Time (h)	T (°C)	Polymer/alumina	T_{m1}	T_{m2}*
1	1.5	4	25	5	141.0	133.0
3	1	1.5	50	10	140.6	131.3
5	2	4	50	25	138.4	127.4
5	2	8	50	32	140.6	130.4
2	2	4	55	90	140.9	130.7
0.35	2	5.5	55	110	142.4	133.6

* For definitions of T_m see text and *Figure 9*

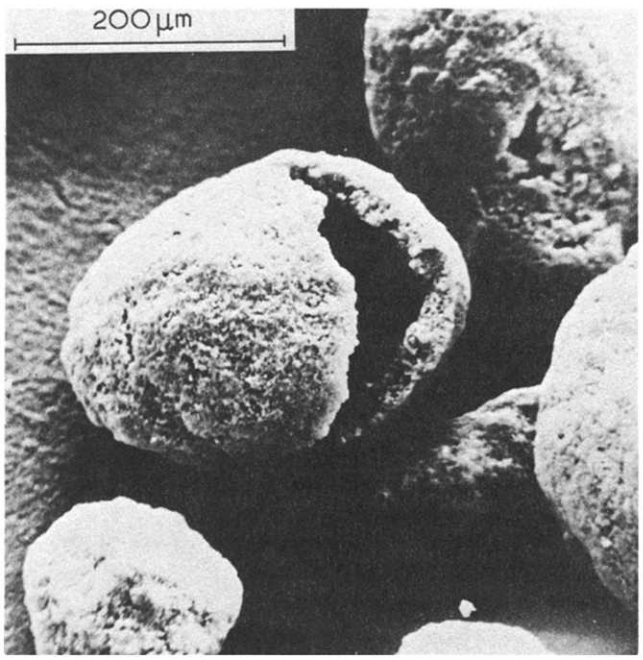

Figure 2 SEM photograph of the hollow polymer beads at a polymer:alumina ratio of 25:1

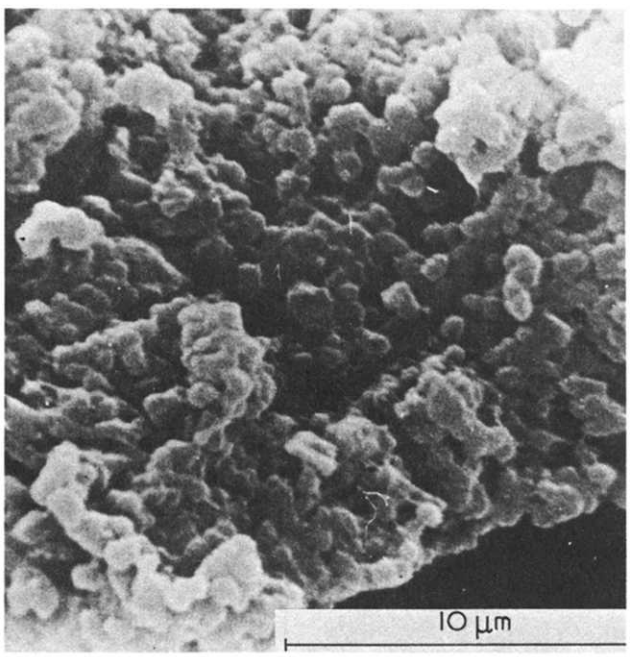

Figure 3 SEM photograph of wall of a polymer bead at polymer:alumina ratio of 10:1

by the dye, suggesting that there is no significant barrier to uniform penetration of the alumina by the initiator during catalyst preparation. In all subsequent experiments the catalyst was produced by titration of alumina with zirconium tetrabenzyl solution until the alumina was saturated as revealed by a permanent yellow colour in the supernatant liquid; the final catalyst was filtered off and washed before use.

Polymerization and morphological studies

Polymerizations were performed in a glass reactor using toluene as the suspension medium. In a typical experiment 200 cm^3 of dried, degassed toluene was used with 1 g of alumina-supported catalyst at a temperature of 50°C. The reaction vessel was pressurized with ethylene to a pressure of 2 atm and was continuously stirred. The activated alumina particles are orange-yellow in colour. They disperse easily into toluene but coagulate rapidly as soon as ethylene is admitted. After about 30 min polymerization the particles become dispersed again and their colour gradually changes to white.

Polymerizations were terminated by addition of methanol and the polymer recovered by filtration. Samples for transmission electron microscopy were prepared by ultrasonic dispersion of a toluene suspension which was then placed on an evaporated film of carbon on a glass slide. After evaporation of the toluene the carbon film was transferred to the copper grids used for sample support. Electron microscopy was performed using either a JEOL JEM-120 C transmission electron microscope or a Cambridge Stereoscan IIA scanning microscope.

Scanning calorimetry was performed using a Perkin–Elmer DSC-2.

RESULTS

Polymer morphology

The yield of polymer in a polymerization experiment is a function of reaction time, temperature, ethylene pressure and concentration of catalyst. *Table 1* lists the yields and conditions for the samples that we examined by electron microscopy, together with their melting points measured by d.s.c. The weight ratios of polymer to alumina ranged from 5 to 110, which would be regarded as low to medium activity in commercial terms[9] although there is no reason to believe that the polymerization had ceased before it was deliberately terminated.

In all cases the polymer was produced as white, hollow spherical beads, as is illustrated in *Figure 2* for a polymer:alumina ratio of 25. At low polymer:alumina ratios, higher magnifications show the walls of the beads to consist of globules of about 0.5 μm diameter in clusters

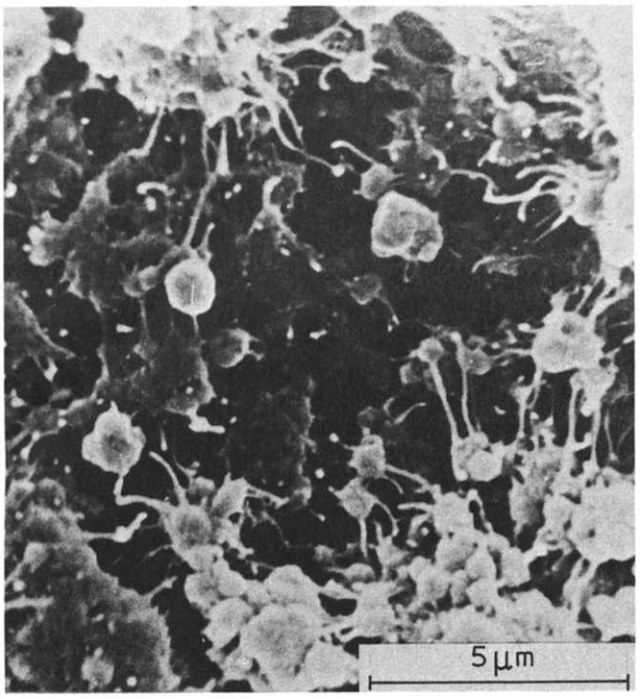

Figure 4 SEM photograph of wall of a polymer bead at a polymer:alumina ratio of 25:1

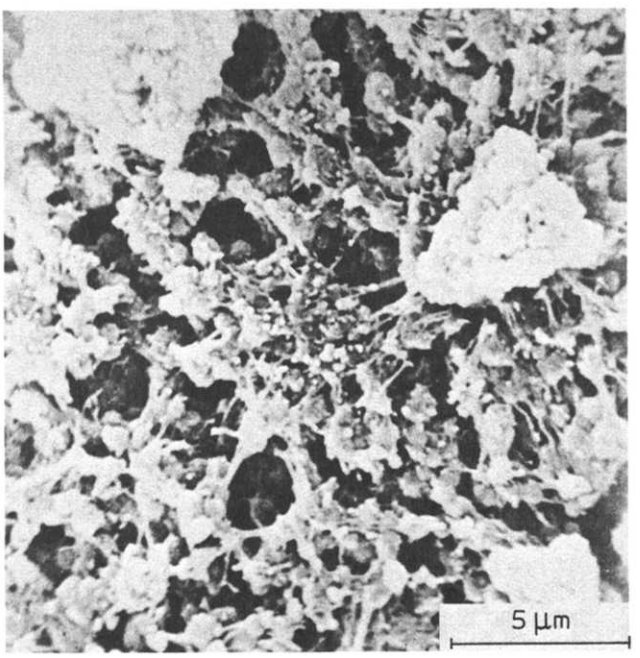

Figure 5 SEM photograph of inner wall of a polymer bead at a polymer:alumina ratio of 110:1

separated by pores, as is shown in *Figure 3* for a ratio of 10. As the polymer:alumina ratio increases, the globules appear as individuals separated by fibres of polymer of the order of 0.2 μm diameter and up to 3 μm long, as shown for a ratio of 25 in *Figure 4*. These fibres are smooth-surfaced cylinders and free ends can often be seen, suggesting that they have been stretched and fractured.

The internal surfaces of the beads always contain clumps of particles which can be identified by EDAX. as being alumina. These particles decrease rapidly in number and size with increasing conversion but are still present even at polymer:alumina ratios of 110, as shown in *Figure 5*. Rough estimates of the size distribution of the polymer beads, derived from optical micrographs, show that the bead size increases with increasing conversion, as illustrated in *Figure 6*; at the same time the thickness of the bead wall increases from around 20 ± 5 μm at a ratio of 10 to around 40 ± 10 μm at a ratio of 90.

In order to allow the individual globules to be examined more clearly, the polymer beads were subjected to ultrasonic dispersion then examined by transmission electron microscopy. At low conversions disruption is facile but it becomes more difficult at higher conversions; after treatment of the beads with fuming nitric acid for 90 min they disperse readily.

Figure 7 shows the transmission micrograph of a single globule, obtained from a polymer:alumina ratio of 10:1. The blob of material to the left of the globule is identifiable by electron diffraction as free alumina and the occurrence

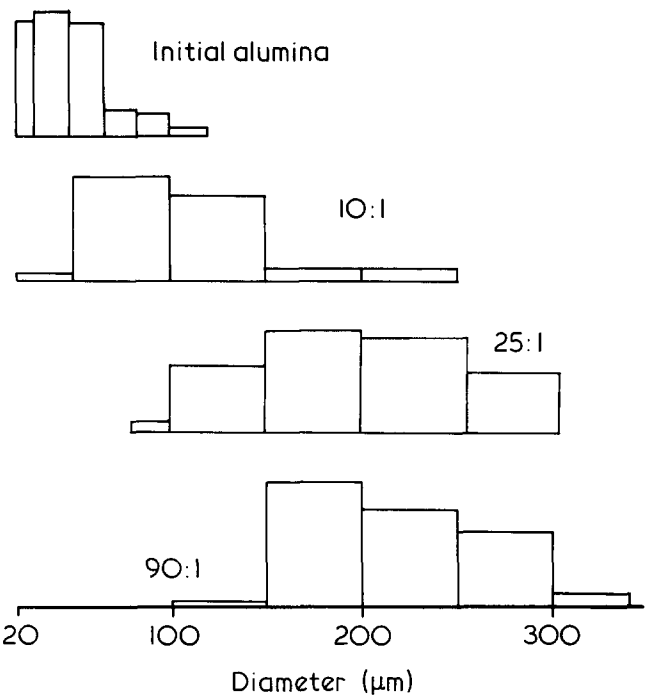

Figure 6 Approximate size distribution for polymer beads of various conversions as measured by optical microscopy

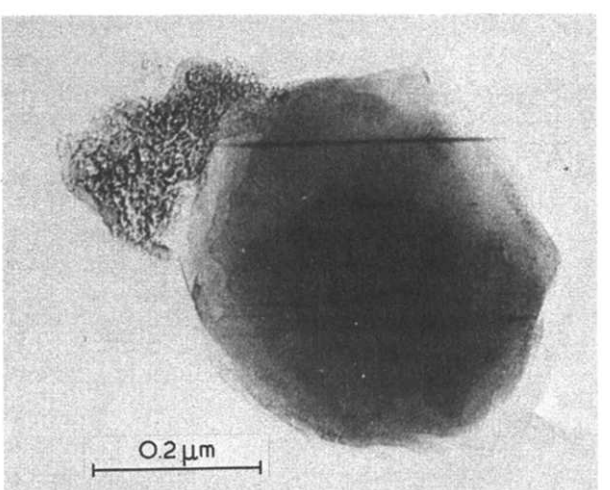

Figure 7 TEM photograph of a single polymer globule obtained by ultrasonic disruption and a polymer:alumina ratio of 10:1

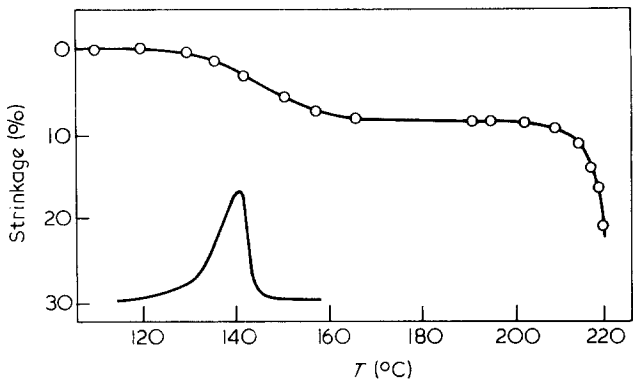

Figure 8 Diametric shrinkage of polymer beads at a polymer:alumina ratio of 90:1. Heating rate 5°C min^{-1}. Inset shows d.s.c. melting thermogram for the same polymer

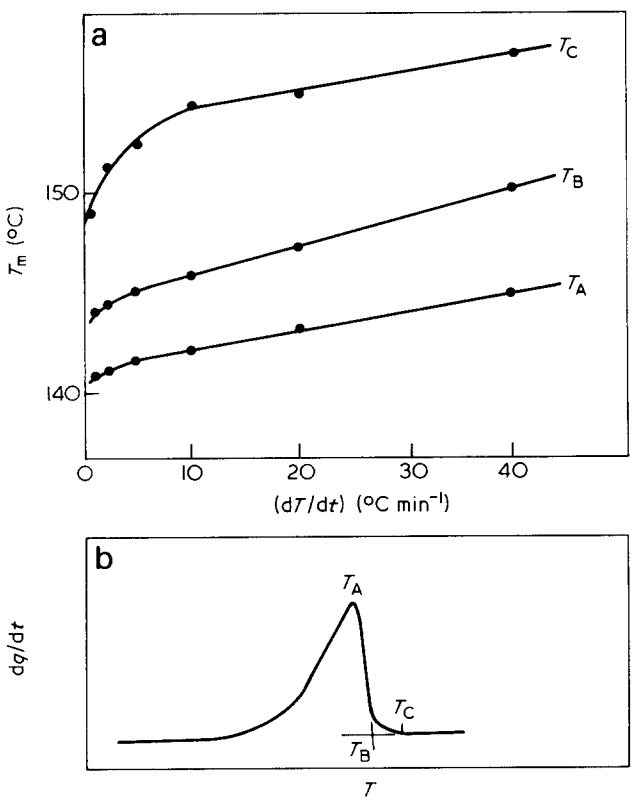

Figure 9 (a) Effect of heating rate on melting temperatures for a typical polymer sample. A d.s.c. thermogram annotated to define the T_m values used. Values quoted in ***Table 1*** correspond to T_A

of such free alumina clusters decreases rapidly with increasing conversion. A region of much higher contrast is observed at the centre of each globule and a number of observations combine to suggest such regions are alumina. On going from a polymer to alumina ratio of 10:1 the globule size increased from 0.4 ± 0.1 μm to 0.6 ± 0.1 μm while the central catalyst fragment decreased from 0.12 ± 0.02 μm to 0.04 ± 0.02 μm. Thus their size decreases markedly with increasing conversion even though the size of the globules increases only slightly. At the same time the central clusters are unaffected by melting of the sample either in the electron microscope or in an oven before microscopy.

Melting behaviour

The melting behaviour of the polymer beads was observed both by d.s.c. and by measuring the diameter shrinkage of the beads as a function of temperature in a hot-stage microscope. *Figure 8* shows the results of both experiments for beads with a polymer:alumina ratio of 90. In all cases the beads remain visibly intact throughout the crystalline melting process and only collapse when they reach temperatures of 180°C or higher, depending upon heating rate. Observations in polarized light at 147°C reveal a small amount of negative birefringence in the beads, which is lost slowly over a period of about 6 h. Similarly, sections prepared by mounting the beads in resin and microtoming show overall, weak negative birefringence, suggesting that the polymer chains are circumferentially oriented within the beads.

All samples showed d.s.c. melting peaks in the range 138°–142°C, which is significantly higher than would be expected for samples crystallized under normal conditions. On recrystallization and remelting the peak shifted to 128°–133°C. *Figure 9* shows the effect of heating rate on the melting temperature for fast melting; the melting temperature increases continuously with heating rate in a way typical of slowly crystallized or oriented structures[17,19]. The maximum melting temperature also increases with the polymer:alumina ratio (see *Table 1*) but this may reflect molecular weight changes since the remelting temperature also changes.

When samples produced at high polymer:alumina ratios are slowly recrystallized a shoulder is seen on the high-temperature side of the crystallization exotherm, as shown in curve A of *Figure 10*, suggesting some retained order in the molten polymer which is able to initiate crystallization. This shoulder disappears slowly on annealing the sample just above the melting point and rapidly if the sample is heated to 175°C. It also disappears rapidly on exposure of the sample to fuming nitric acid, a treatment which rapidly lowers the first melting peak of the polymer but has little effect on remelting.

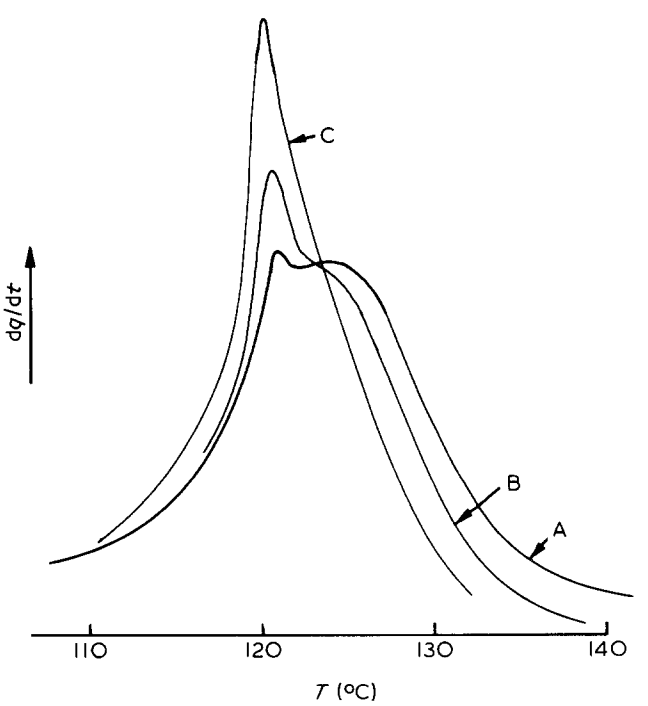

Figure 10 Effect of annealing of molten polymer on its recrystallization exotherm. Curve A, annealed at 142°C for 15 min; curve B, annealed at 144°C for 15 min; curve C, annealed at 177°C for 1 min

DISCUSSION

One of the most significant observations we have made is that polymerizations under the conditions that we used invariably gives rise to hollow spherical beads of polymer formed on the initial spherical alumina aggregates. This observation shows that the rate of polymerization cannot be uniform throughout the initial particle and two explanations are possible. It is possible that the non-uniformity of reaction rate reflects a non-uniform distribution of the catalyst centres or that it reflects diffusional limitations on the rate of reaction. Murray[14] observed the formation of hollow beads on similar catalysts when the catalyst was prepared by addition of the zirconium benzyl solution to the alumina. He concluded that this reflected non-uniform distribution of catalyst and was able to show, by electron probe microanalysis, that the zirconium atoms were concentrated in the surface layers of the particles of alumina; preparation of the catalyst by addition of alumina to the zirconium solution gave a more uniform distribution and polymerization which did not yield hollow spheres. We do not believe that this explanation is valid for our experiments. The catalysts used by Murray were prepared with a specific loading of metal, less than the amount required to react with all available hydroxyl groups. Under these conditions the very high reactivity of the metal alkyl towards hydroxyl groups makes it difficult to avoid non-uniform distribution of the metal. In our case the catalysts were all fully saturated by the metal alkyl. Reactions were performed until the supernatant liquid permanently retained the yellow colour of the metal complex, implying that no more would react with the alumina. This procedure, allied with the observation that large organic dye molecules can readily dye the particles uniformly, implies that the metal was distributed uniformly throughout the initial catalyst particle and that the formation of hollow spheres is the result, in our case, of diffusion control.

The morphology of a polymer is invariably determined by the kinetics of its crystallization since the relatively low mobility of polymer molecules prevents the formation of the near-equilibrium structures seen when small molecules are crystallized from solution. In a heterogeneous polymerization the variety of complex morphologies which can be observed must be partly determined by the non-uniform concentration of monomer and polymer that results from the interaction of diffusion, polymerization and polymer precipitation. Crabtree *et al.*[19] have discussed the role of diffusional processes in the kinetics of Zeigler–Natta polymerization and have shown that fairly simple diffusional models can be used to fit the observed time dependence of the rate of polymerization. Following these authors we can identify four diffusion barriers which may contribute to the kinetics: (1) transfer of monomer from the gas phase into the solvent, (2) diffusion of monomer from the solvent into the macroscopic polymer–catalyst aggregate forming each individual polymer particle, (3) diffusion of monomer into the primary catalyst particle and (4) diffusion of the product polymer away from the site of its production. The idea that one or more of these diffusion processes controls the morphology of the product polymer particles is suggested by the surprising uniformity in the morphologies produced by a wide variety of catalyst systems as described earlier. Thus the polymer globules of about 0.5 μm diameter that we observe have been seen in many polymerization systems, mainly at low polymer:catalyst ratios, whilst worms of about 0.5 μm diameter are very commonly observed at higher conversion[1,5]. It is therefore worth while to examine the diffusion processes in more detail.

It is well known that commercial polymerization using highly active catalysts in high load slurry processes can consume ethylene faster than it can be fed into the polymerization reactor so that transfer into the liquid phase is the rate-limiting factor[20]. Boocock and Haward[21] assumed that the rate of polymerization is first order in catalyst concentration and in the actual concentration of monomer at the surface of the catalyst particle and that this latter concentration is determined by the diffusion of monomer from the gas phase. They showed that the rate of monomer consumption, R, should be given by an expression of the form:

$$1/R = 1/\alpha[\mathrm{Ti}]C_o + 1/\beta A C_o \qquad (1)$$

where C_o is the saturation content of monomer in the solution, α is a constant determined by the kinetics of the polymerization, β is the mass transfer coefficient for monomer from gas to liquid phase and A is the interface area, which depends upon the reactor design and the agitation. This relation predicts a linear dependence of $1/R$ upon $1/[\mathrm{Ti}]$, whose intercept gives the maximum rate at which monomer can be transferred into the solvent under given conditions of agitation. According to Boocock and Haward, equation (1) adequately describes the polymerization of ethylene by their Ziegler–Natta catalyst and the limiting rates of mass transfer calculated from the polymerization kinetics agree quite well with measurements made in the absence of catalyst.

Although interphase mass transfer is important for the high concentrations of highly active catalyst employed commercially, we do not believe that it is important in our systems. We have worked under conditions where the activity of the catalyst is relatively low and its concentration very much lower than that used commercially. Experimentally we find that a 10-fold reduction in catalyst concentration produces a 10-fold decrease in polymerization rate under our conditions, implying that the second term in equation (1) is small relative to the first, leading to simple first-order, diffusion-free behaviour.

In concluding that, for our experiments, monomer diffusion into the solvent presents no barrier to polymerization, we imply that the monomer concentration in the solvent is uniform and equal to the saturation concentration at the partial pressure of monomer used. At the beginning of the reaction this must also be the concentration at the catalyst surface, but one can reasonably enquire how far this concentration will be affected by the formation of polymer. According to Ballard[11], polymerization of ethylene on the initiators used by us in our work has a high initial rate which decreases by about 30% in the first 2 h of reaction, then remains essentially constant for long periods. Ballard interprets this behaviour as implying that the precipitation of polymer leads to a diffusional barrier to polymerization, which, once established, is constant throughout the reaction. However, we have observed[22] very similar behaviour when either propylene or butadiene is polymerized with the same initiator. Since in both of these cases the polymer is soluble in the reaction solvent, diffusion limitation is unlikely and we believe that the behaviour is due to the presence of a fraction of

Table 2 Calculated diffusional efficiencies for model particles*

Particle	D ($cm^2\ s^{-1}$)	a (μm)	C_0 ($mol\ l^{-1}$)	k (s^{-1})	F/F_0
Initial alumina	1.7×10^{-5}	20	0.027	11	0.86
Initial alumina – pores filled with swollen PE	1.3×10^{-6}	20	10^{-2}	200	0.11
Particle with 10 g PE/g (swollen)	4.4×10^{-6}	60	3.5×10^{-2}	0.3	0.85
Particle with 10 g PE/g (unswollen)	1×10^{-7}	60	9.6×10^{-3}	42	0.025
Particle with 10 g PE/g (swollen and drawn)	8×10^{-8}	60	4.3×10^{-3}	250	9×10^{-3}

* Using equations in text and parameters estimated in appendix

initiating sites on the alumina surface which are more active than the others but which gradually decay in activity or become destroyed as the reaction proceeds. Active site decay is well documented in Ziegler–Natta chemistry[1]. For example, Begley[23], studying propylene polymerization by Ziegler–Natta catalysts, suggested that the observed fall in rate with time is due to active site decay and that monomer diffusion is unimportant. More recently, Crabtree *et al.*[19] suggested that both catalyst decay and monomer diffusion are required to explain the observed rate decay during propylene polymerization; using a model in which the polymerization is assumed to take place independently on spherical subparticles of catalyst, together with a first-order decay of catalyst activity, they obtain good fits for experimental rate–time profiles. In contrast, Yermakov and Zakharov[24] considered polymerization of ethylene on alumina-supported catalysts as involving porous assemblies of subparticles. They concluded that diffusion restriction at the primary particle level is unimportant and that monomer diffusion into the aggregate of subparticles will be significant only at extremely high rates of polymerization. Because there is so much disagreement on the importance of diffusion we have attempted to analyse the problem for our catalyst system, bearing in mind that the diffusional behaviour of catalyst particles can be expected to change significantly as they are fragmented during polymerization.

Diffusion of a reactant into an initial spherical catalyst bead or into a solid sphere of catalyst and polymer is mathematically analysable if reaction within the sphere follows first-order kinetics. In that case, the steady-state flux of monomer into a sphere of radius a is given by [25]:

$$F = 4\pi a D C_0 [(ka^2/D)^{1/2} \coth\{(ka^2/D)^{1/2}\} - 1] \quad (2)$$

where D is the diffusion coefficient, C_0 is the surface concentration of monomer in the bead, k is the apparent first-order rate constant for the polymerization and is equal to $k'[S]$, where the rate of polymerization is $k'[S][M]$ and $[S]$ is the concentration of active sites in the polymerization at any time. Values of k are not measurable without assumptions about values of D and C_0. However, since F is calculable from the polymerization rate, k can be calculated if D and C_0 are known. In the absence of any diffusional restriction ($D = \infty$), the monomer flux is given by:

$$F_0 = 4\pi a^3 C_0 k/3 \quad (3)$$

and the ratio F/F_0 can be considered as an efficiency. If this ratio is close to unity then polymerization will proceed uniformly throughout the bead, which would be expected to produce a uniformly expanding solid bead of polymer and catalyst. If F/F_0 is much less than 1, then diffusion is important and the reaction will proceed faster on the outside of the bead than inside; the fact that we observe hollow beads suggests that this situation applies at least at some stage in the reaction.

Using literature data plus some assumptions we have estimated values of D and C_0 for ethylene at 55°C in toluene, in pure polyethylene, in polyethylene swollen with toluene and in swollen polyethylene after drawing. The procedures that we adopted are outlined in the appendix. The density of γ-alumina is 3.5–3.9 $g\ cm^{-3}$ and we assume this figure to be reduced to 2.5 $g\ cm^{-3}$ by the effect of the 30% pore volume of our catalyst particles. Using the estimated values of D and C_0, together with an average flux of monomer, we can compute values for k and for the ratio F/F_0, and these values are presented in *Table 2* for some representative cases. These data suggest that the initial catalyst bead, whose pores contain no polymer, presents little barrier to the polymerization at these rates. However, as soon as the pores become filled with polymer, in the first few minutes of reaction, the efficiency drops to a low value, polymerization becomes very non-uniform and will occur much faster on the outside of the beads than on the inside. Hence unreacted alumina is found inside the hollow polymer beads. Our calculations suggest that two effects may contribute to the further behaviour of the reaction. As the bead is expanded by an increasing volume fraction of swollen polymer, diffusion is more rapid and the efficiency rises. However, as the polymer is drawn by the continued polymerization in the globules around the catalyst subparticles, the diffusion coefficient decreases again, which tends to retard the polymerization rate in those globules that have achieved highest conversions. In view of the assumptions inherent in this model we do not attach significance to the values of k and would certainly not attempt to interpret the variation in k in terms of a polymerization mechanism. According to Ballard[9] the value of k' is $2.2 \times 10^4\ l\ mol^{-1}\ s^{-1}$ at 80°C. Under our conditions, allowing for the fact that only about 1% of the available catalyst sites are active, [S] is of the order of $2 \times 10^{-4}\ mol\ l^{-1}$, giving a k value of around $1\ s^{-1}$ at 80°C. The order-of-magnitude agreement with our values (*Table 2*) is encouraging.

From this discussion we conclude that the formation of hollow spheres is a consequence of diffusion control in the early stages of the polymerization, leading to more rapid reaction on the particle surface. If this were maintained the outer layer would continue to expand more rapidly, stretching the inner layers so that the shell wall should become thinner with time or at least maintain constant thickness. In fact we find that the wall thickness increases with conversion such that the ratio of wall thickness to particle diameter is roughly constant, suggesting that

polymerization is fairly uniform throughout the catalyst particle after the initial non-uniform growth. This implies that polymerization in the inner parts of the particle accelerates relative to that in the outer parts with increasing conversion, possibly due to a diffusion limitation of the monomer concentration on the subparticles with increasing conversion; whatever its cause the faster growth of the inner particles leads to fissuring and rupture of the outer layers.

The diffusion of monomer into a globule of polymer with a catalyst subparticle at its centre can be regarded as a case of diffusion into a hollow sphere, for which the polymerization flux is given by[25]:

$$F = 4\pi D C_0 (1/a - 1/b + 3D/ka^3)^{-1} \quad (4)$$

where b is the radius of the polymer sphere and a is the radius of the catalyst subparticle. Setting D infinitely high allows us to compute the diffusional efficiency F/F_0 as:

$$\frac{F}{F_0} = \frac{3D}{ka^3}\left(\frac{1}{a} - \frac{1}{b} + \frac{3D}{ka^3}\right)^{-1} \quad (5)$$

In our system the individual subparticles of alumina have a mean diameter of around 0.4 μm and are present in very large numbers (around 10^{12} subparticles per gram of alumina) so that the monomer flux into each subparticle is very small. The combination of very small particles and low monomer flux means that all plausible values of D as used in *Table 2* lead to values of F/F_0 close to unity and we conclude that there can be no simple diffusion limitation of the polymerization rate. However, there are other ways in which the polymer may act to reduce the polymerization rate. Thus as the environment around the catalyst particle changes from toluene to swollen drawn polyethylene, the solubility of both ethylene and toluene within the globule will fall significantly and so the monomer concentration at the catalyst surface will fall. At the same time the high viscosity of the polymer capsule increases the difficulty of diffusing newly created polymer segments away from the active sites and may be expected to increase the activation energy for propagation and hence reduce k. None of these effects implies diffusion control at the subparticle level; instead they imply that the effect of the encapsulation of a subparticle is to reduce the polymerization rate relative to that of the free particle, so allowing the reaction to transfer to the unencapsulated subparticles.

At several points in this discussion we have invoked the effect of drawing in reducing both monomer diffusion and solubility in polyethylene. Such drawing would be expected to result from the volume expansion during polymerization; a polymer:alumina weight ratio of 10 is equivalent to a volume expansion of 25, which is equivalent to a biaxial draw ratio of about 3 in the outer layer of a uniform sphere. This drawing is really the result of the fact that the polymer is synthesized much faster than its very low diffusion coefficient will allow it to diffuse away from the catalyst and there is ample evidence that drawing does occur in our system. The melting characteristics of the as-formed polymer are a high melting temperature by d.s.c., a rapid increase in melting temperature with d.s.c. heating rate (superheating), delayed loss of birefringence and order in the melt and a rapid regression to normal behaviour on nitric acid oxidation. The observation of high melting temperatures and superheating in polyethylene is usually associated with the presence of 'extended-chain' crystals formed at very low supercooling or high pressures. However Cappaccio and Ward[26] have reported similar behaviour in polyethylene highly drawn at 75°C. Czorny and Wunderlich[27] have observed effects like those in our polymer, in 'shish-kebabs', highly oriented crystalline fibres formed from hot solutions. They attributed the delayed loss of birefringence and sensitivity to nitric acid to oriented amorphous regions, which restrict the rate of relaxation on melting. Thus the melting results for the nascent polymer are consistent with a highly drawn polymer with oriented interlamellar amorphous regions. The fact that the drawing occurs by swelling of the globules from their centre also limits the ability of the material to shrink and as a result the chain cannot relax to a randomly coiled state until the whole chain has been freed from the crystalline regions. The nitric acid treatment cuts the chains in the amorphous regions so that each crystal can melt and the chains relax independently. The overall negative birefringence of the whole bead shows that some drawing occurs around the circumference of the bead as well as the high degree of drawing within the individual globules.

CONCLUSIONS

The morphology of a polymer particle, formed under conditions where the polymer is forced to precipitate from the reaction medium, is determined, in a complex way, by the interaction of the primary catalyst morphology, the rate of polymerization and the effect of polymer formation on that rate and by the properties of the polymer produced. Polymerization of ethylene on our alumina-supported catalyst is found to have many morphological features in common with polymerization of ethylene and propylene on other catalyst systems. We believe that the development of the final morphology in our particular system occurs as follows:

(a) Polymerization initially occurs rapidly throughout the catalyst particle; a polymer:alumina ratio of about 0.1 is achieved in a few minutes and at this point the pores in the alumina are filled with swollen polyethylene.

(b) Once the pores are filled, polymerization occurs most rapidly on the outside of the particle, which expands; this expansion in the outer layer leads to formation of a hollow sphere with relatively unreacted catalyst stuck to the inner surface.

(c) Encapsulation of subparticles in the outer layer by globules of polymer, with simultaneous drawing, leads to a decrease in the rate of polymerization in the outer layer. This allows monomer to penetrate further into the hollow bead where polymerization causes fissuring and rupture of the outer layers, allowing even easier access for monomer.

(d) The expansion and drawing in the globules leads to a decrease in toluene swelling of the polymer. The beads then stop clumping and separate. As the process proceeds there is a great deal of drawing as clumps of subparticles are pulled apart. This drawing produces thin (0.1–0.6 μm) fibres, containing catalyst subparticles; these fibrils continue to polymerize and to be drawn and they may fracture.

(e) The fact that capsule formation and drawing slows

growth and that the radial growth rate of the globular particles will decrease with increasing size (for a constant polymerization rate) leads to relatively uniformly sized globules and worms. This whole cycle can continue more or less indefinitely as long as the swelling forces set up in the particle lead to expansion and drawing.

It is worth while to emphasize that the development of this structure is dependent upon the ratio of polymerization rate to monomer diffusion rate. The differences between our system and the structures reported by Murray[14] almost certainly reflect this fact; in particular it is noteworthy that a similar catalyst with a lower metal loading did not give rise to hollow particles[14] and it is expected that more rapid diffusion or slower polymerization will lead to more compact particles whereas more rapid polymerization would be expected to lead to a mass of disintegrated granules. At the same time the drawing behaviour and the development of worms are both expected to be sensitive to the molecular weight of the polymeric product.

Murray has also pointed out[14] that the exact morphology produced by these catalysts is sensitive to the grade of support material that is used and particularly to the ease or difficulty of mechanical disruption.

ACKNOWLEDGEMENTS

We thank the Government of Turkey for a maintenance grant for A.A Thanks are also due to Mr L. Ardley for much assistance with electron microscopy, to ICI Petrochemicals and Plastics Division for the gift of ethylene monomer and to Dr R. T. Murray for helpful discussions during the preparation of this paper.

APPENDIX

Estimation of data used in generating Table 2

Diffusion of ethylene in toluene. There is apparently no literature value. However, for ethane in heptane[28] at 30°C, $D = 5.6 \times 10^{-5}\ cm^2\ s^{-1}$. The viscosity of toluene at 55°C (0.406 cP) is almost identical to that of heptane[28] at 30°C, so we take $D = 5.6 \times 10^{-5}\ cm^2\ s^{-1}$ for ethylene in toluene at 55°C.

Solubility of ethylene in toluene. According to Hildebrand and Scott[29] the saturation pressure for ethylene dissolving in toluene is 50.5 atm at 9.9°C and 65.79 atm at 25°C. Extrapolation gives a value of 103.9 atm at 55°C corresponding to a mole fraction of ethylene of 9.6×10^{-3} at 1 atm pressure (assuming ideality). Since the density of toluene at 55°C is 0.85, the solubility of ethylene is $0.089\ mol\ l^{-1}\ atm^{-1}$.

Solubility and diffusion of ethylene in polyethylene. According to Michaels and Bixler[30,31] the diffusion coefficient of ethylene in polyethylene at 55°C is $1.03 \times 10^{-7}\ cm^2\ s^{-1}$ and the solubility is $9.6 \times 10^{-3}\ mol\ l^{-1}\ atm^{-1}$. We measure the swelling of polyethylene by toluene to be 0.119 g/g polymer and 0.153 g/g polymer at 55°C. The solubility of gases in swollen polyethylene can be represented by[32]:

$$S = S_0 \exp(\sigma c)$$

where σ is a constant, equal in this case to 2.2, c is the concentration of solvent in g/g amorphous polymer and S_0 is the solubility in unswollen polymer. This gives a solubility of ethylene in toluene swollen polyethylene of $3 \times 10^{-2}\ mol\ l^{-1}\ atm^{-1}$. The diffusion coefficient can likewise be expressed as:

$$D = D_0 \exp(\gamma c)$$

where γ is a constant, equal to 21.4, giving a diffusion coefficient of ethylene in swollen polyethylene of $2.7 \times 10^{-6}\ cm^2\ s^{-1}$ at 55°C. The effect of drawing on these properties has been measured by Peterlin and coworkers for methylene chloride swollen polyethylene[33,34]. From their results 10-fold drawing is found to reduce the solubility 8-fold and the expected diffusion coefficient at 55°C in drawn, swollen polyethylene is thus $6.5 \times 10^{-8}\ cm^2\ s^{-1}$.

REFERENCES

1 Boor, J. Jr 'Ziegler–Natta Catalysts and Polymerizations', Academic Press, New York, 1979, Ch. 8
2 Chanzy, H. D., Fisa, B. and Marchessault, R. H. *Crit. Rev. Macromol. Sci.* 1973, **1**, 315
3 Baker, R. T. K., Harris, P. S., White, R. J. and Roper, A. N. *J. Polym. Sci.* 1973, **11**, 45
4 Revol, J. F., Luk, W. and Marchessault, R. H. *J. Crystal Growth* 1980, **48**, 240
5 Wristers, J. *J. Polym. Sci., Phys.* 1973, **11**, 1801
6 Graf, R. J. L., Kortleve, G. and Vonk, C. G. *J. Polym. Sci. B* 1970, **8**, 735
7 Chanzy, H. D., Revol, J. F., Marchessault, R. H. and Lamade, A. *Kolloid Z. Polym.* 1973, **251**, 563
8 Davidson, T. *J. Polym. Sci. B* 1970, **8**, 855; *Polym. Prepr.* 1971, **12**, 478
9 Ballard, D. G. H. *Adv. Catal.* 1973, **23**, 293
10 Ballard, D. G. H., Jones, E., Pioli, A. J. P., Robinson, P. A. and Wyatt, R. J. Br. Patent 1314828, 1973
11 Ballard, D. G. H. *J. Polym. Sci., Chem.* 1975, **13**, 2191
12 Ballard, D. G. H., Jones, E., Wyatt, R. J., Murray, R. T. and Robinson, P. A. *Polymer* 1974, **15**, 169
13 Murray, R. T., Ballard, D. G. H. and Platt, D. Proc. 6th Eur. Congr. on Electron Microscopy, Jerusalem, 1976, p. 393
14 Murray, R. T. in 'Characterization of Catalysts' (Eds. J. M. Thomas and R. M. Lambert), Wiley, New York, 1980, p. 105
15 Giannini, U. and Zucchini, U. *J. Chem. Soc. Chem. Commun.* 1968, 940
16 Wade, K. and Banister, A. J. in 'Comprehensive Inorganic Chemistry', vol. 1, Pergamon, New York, 1973, p. 1033
17 Helmuth, E. and Wunderlich, B. *J. Appl. Phys.* 1965, **36**, 309
18 Perkins, W. G. and Porter, R. S. *Polym. Eng. Sci.* 1976, **16**, 200
19 Crabtree, J. R., Grimsby, F. N., Nummelin, A. J. and Sketchly, J. M. *J. Appl. Polym. Sci.* 1973, **17**, 959
20 Vandenberg, E. J. and Repka, B. C. in 'Polymerization Processes' (Eds. C. E. Schildknecht and I. Skeist), Wiley, New York, 1977
21 Boocock, G. and Haward, R. N. *S.C.I. Monograph No. 20*, Soc. Chem. Ind., London, 1965, p. 3
22 Courtis, A. D.Phil. Thesis, University of Sussex, 1976
23 Begley, J. W. *J. Polym. Sci. A* 1966, **4**, 319
24 Yermakov, Yu. and Zakharov, V. *Adv. Catal.* 1975, **24**, 173
25 Crank, J. 'The Mathematics of Diffusion', 2nd edn., Oxford University Press, London, 1975
26 Clements, J., Cappaccio, G. and Ward, I. M. *J. Polym. Sci., Phys.* 1979, **17**, 693
27 Czorny, C. and Wunderlich, B. *Makromol. Chem.* 1977, **178**, 843
28 'Handbook of Chemistry and Physics' (Ed. R. C. Weast), 56th Edn., C.R.C. Press, 1975
29 Hildebrand, J. H. and Scott, R. L. 'Regular Solutions', Prentice-Hall, Englewood Cliffs, NJ, 1962
30 Michaels, A. S. and Bixler, H. J. *J. Polym. Sci.* 1961, **50**, 393
31 Michaels, A. S. and Bixler, H. J. *J. Polym. Sci.* 1961, **50**, 413
32 Rogers, C. E., Stannett, V. and Swzarc, M. *J. Polym. Sci.* 1960, **45**, 61
33 Peterlin, A., Williams, J. L. and Stannett, V. *J. Polym. Sci. A-2* 1967, **5**, 957
34 Williams, J. L. and Peterlin, A. *J. Polym. Sci. A-2* 1971, **9**, 1483